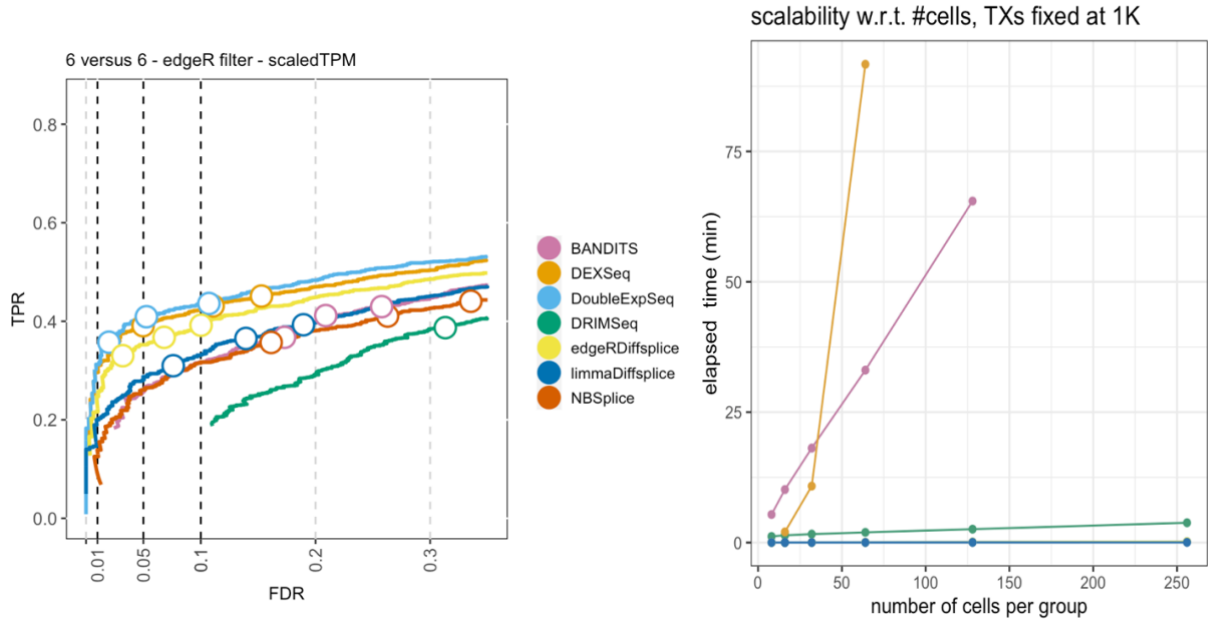


1 Supplementary Figures

2



3

4 **Figure S1: Performance and scalability evaluation on a subset of the Love et al. dataset.** To allow for a
5 performance and scalability evaluation of BANDITS, which does not scale to datasets with a large number of
6 transcripts, we here perform a DTU analysis for the *6 versus 6* samples dataset of Love et al. with only 1000
7 transcripts. **Left panel: performance evaluation.** The results are in line with those of Figure 1A. The performance
8 of BANDITS is indicated in pink. **Right panel: Scalability evaluation.** BANDITS scales linearly with respect to the
9 number of cells (or samples) in the dataset. The slope of the linear trend, however, is considerably larger than
10 those of the other DTU methods that scale linearly. Note that the profiles of limma diffsplice, edgeR diffsplice
11 and DoubleExpSeq overlap in this figure.

12

13

14

15

16

17

18

19

20

21

22

23

24

25

26

27

28

29

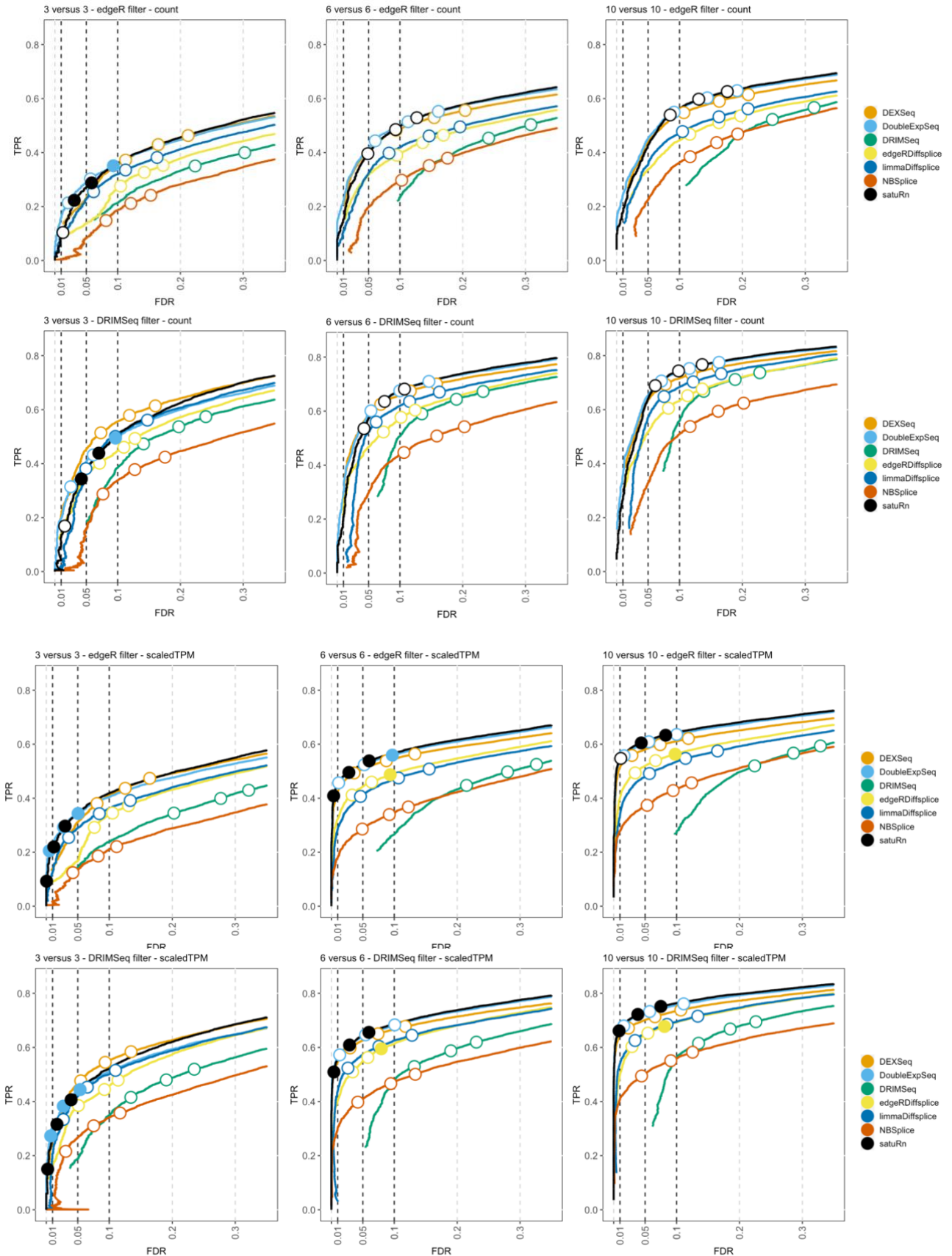
30

31

32

33

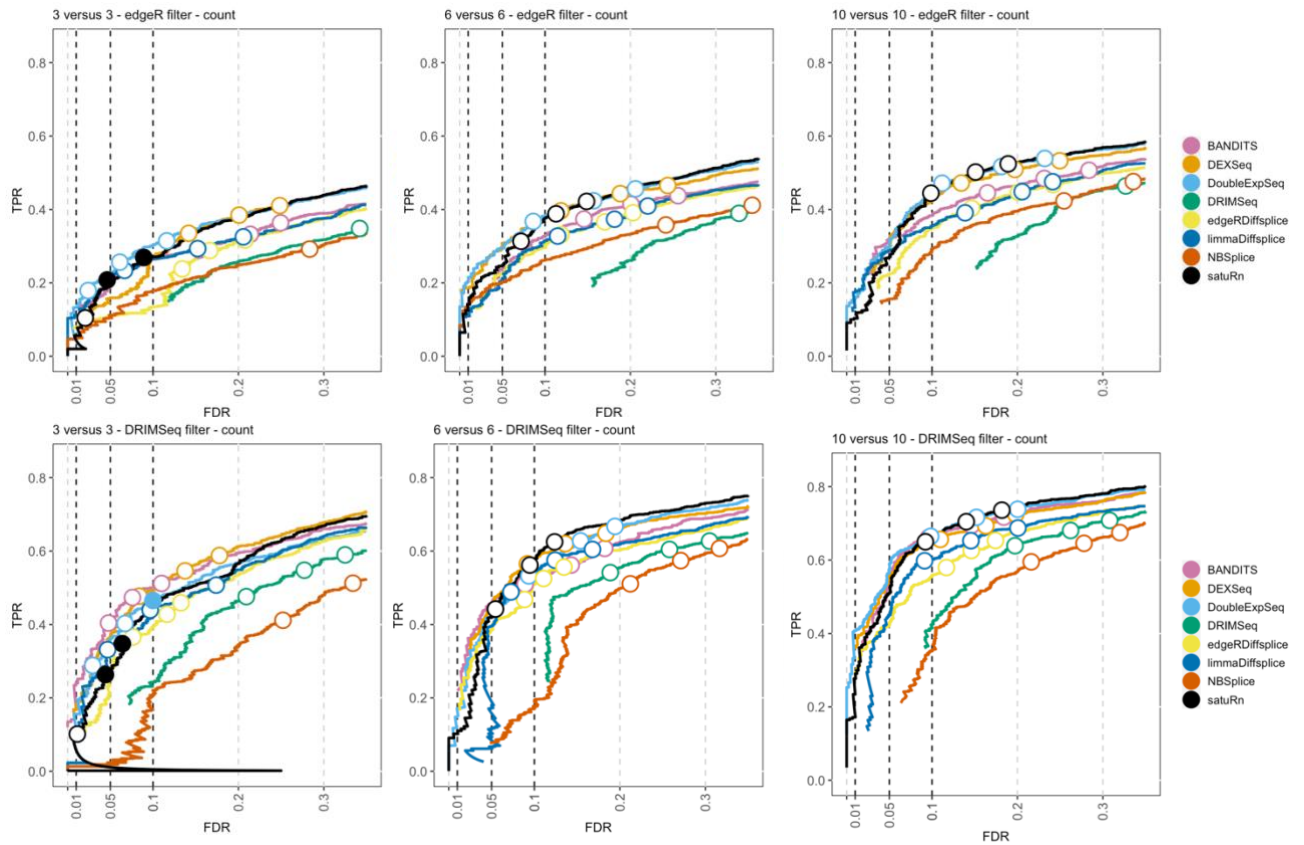
34



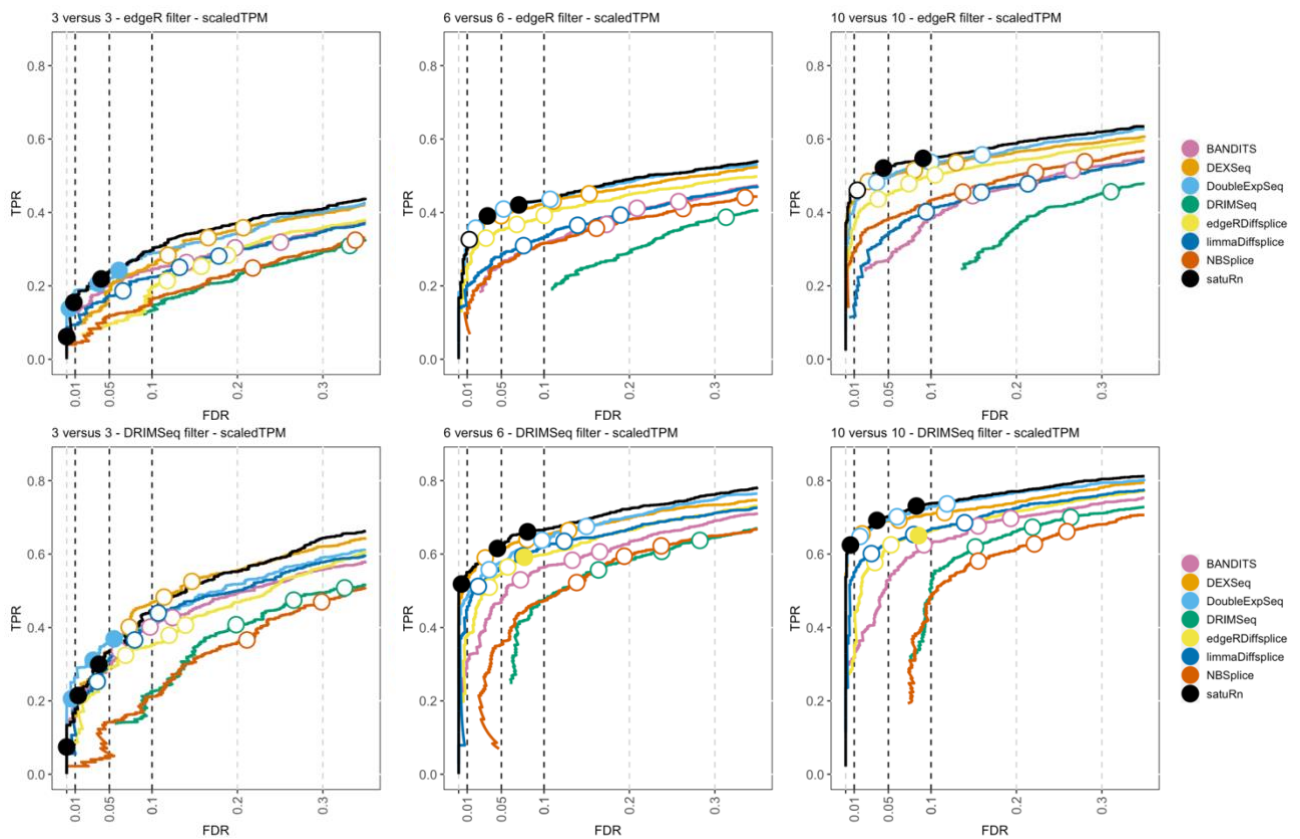
36 **Figure S2: Performance evaluation of satuRn on different subsamples of the simulated bulk RNA-Seq dataset**
 37 **by Love et al.** FDR-TPR curves visualize the performance of each method by displaying the sensitivity of the
 38 method (TPR) with respect to the false discovery rate (FDR). The three circles on each curve represent working

39 points when the FDR level is set at nominal levels of 1%, 5% and 10%, respectively. The circles are filled if the
40 empirical FDR is equal or below the imposed FDR threshold. We subsampled two-group comparisons according
41 to three different samples sizes; a *3 versus 3*, *6 versus 6* and *10 versus 10* comparison, as denoted in the panel
42 titles. The benchmark was performed both on the raw counts (**rows 1 and 2**) or on scaled transcripts-per-million
43 (TPM) (**rows 3 and 4**) as imported with the Bioconductor R package tximport¹. We additionally adopted two
44 different filtering strategies: an edgeR-based filtering (**rows 1 and 3**) and a DRIMSeq-based filtering (**rows 2 and**
45 **4**). Overall, the performance of satuRn is on par with those of the best tools in the literature, DEXSeq and
46 DoubleExpSeq. In addition, satuRn achieves a better control of the FDR on all datasets. For extremely small
47 sample size, i.e. the *3 versus 3* comparison, the performance is slightly below that of DEXSeq, and inference does
48 become slightly too conservative. Note that, as expected, the performances increase with increasing sample
49 size, and a higher performance is achieved with the more stringent DRIMSeq filtering criterion (see Methods),
50 which goes at the cost of retaining fewer transcripts for DTU analysis. Finally, we note that the performances
51 and FDR control are consistently higher for the scaled TPM data as compared to the raw counts. Note that this
52 was only observed for this particular dataset.

53
54
55
56
57
58
59
60
61
62
63
64
65
66
67
68
69
70
71
72
73
74
75
76
77
78
79
80
81
82
83
84
85



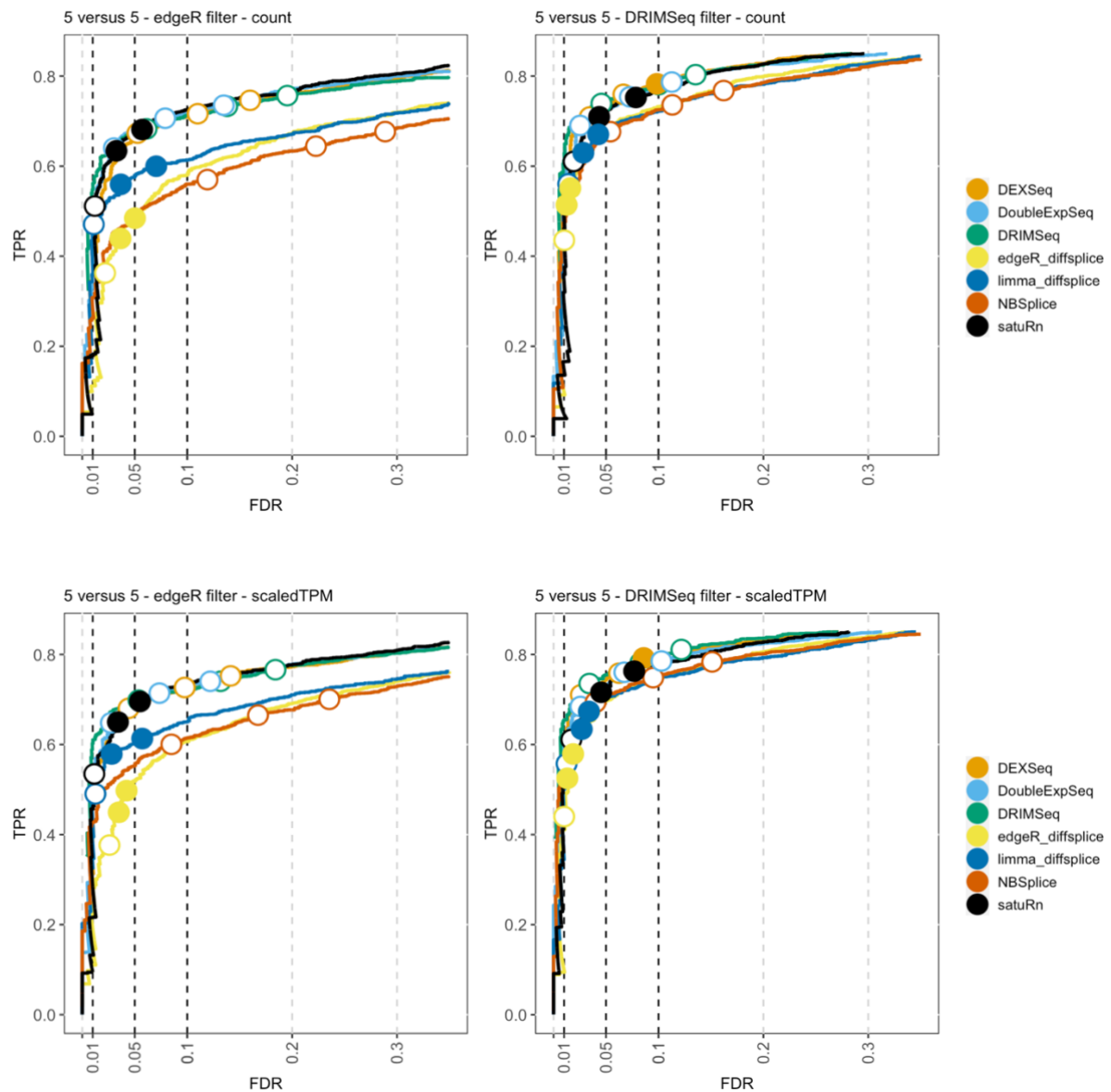
86



87 **Figure S3: Performance evaluation on different subsamples of the simulated bulk RNA-Seq dataset by Love et**
 88 **al. with a reduced number of transcripts to allow for a comparison with BANDITS. FDR-TPR curves visualize the**
 89 **performance of each method by displaying the sensitivity of the method (TPR) with respect to the false discovery**

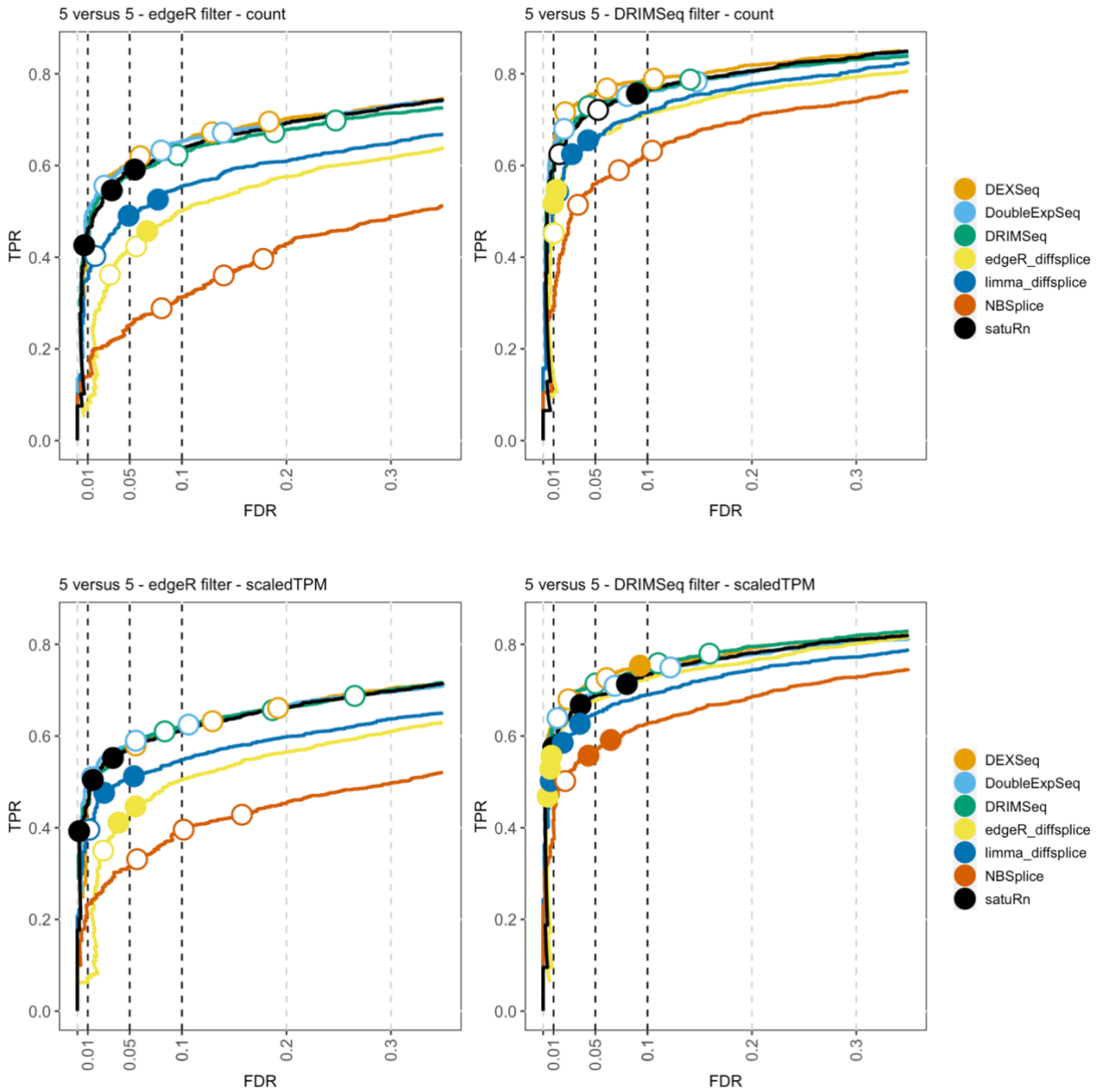
90 rate (FDR). The three circles on each curve represent working points when the FDR level is set at nominal levels
91 of 1%, 5% and 10%, respectively. The circles are filled if the empirical FDR is equal or below the imposed FDR
92 threshold. We subsampled two-group comparisons according to three different samples sizes; a *3 versus 3*, *6*
93 *versus 6* and *10 versus 10* comparison, as denoted on top of the panels. The benchmark was performed both on
94 the raw counts (**rows 1 and 2**) or on scaled transcripts-per-million (TPM) (**rows 3 and 4**) as imported with the
95 Bioconductor R package tximport¹. We additionally adopted two different filtering strategies: an edgeR-based
96 filtering (**rows 1 and 3**) and a DRIMSeq-based filtering (**rows 2 and 4**). Note that, in contrast to Figure S2, we
97 additionally randomly subsampled 1000 genes (~3000-5000 transcripts) after filtering, in order to reduce the
98 number of transcripts in the data and thereby allowing for a DTU analysis with BANDITS. In concordance with
99 Figure S2, the performance of satuRn is on par with the best tools of the literature with a better control of the
100 FDR in general. While the performance of BANDITS is good for the settings for which it was originally developed,
101 (i.e., small datasets with a stringent filtering criterium), its performance is reduced in larger, more leniently
102 filtered datasets and inference is also overly liberal in these settings. In addition, while all other methods perform
103 much better on the scaledTPM data (rows 3 and 4) than on the raw count data (rows 1 and 2), BANDITS has a
104 similar performance on both input data types. This can be explained by the fact that BANDITS inherently corrects
105 for differences in transcript length, even when raw counts are used as an input.

106
107
108
109
110
111
112
113
114
115
116
117
118
119
120
121
122
123
124
125
126
127
128
129
130
131
132
133



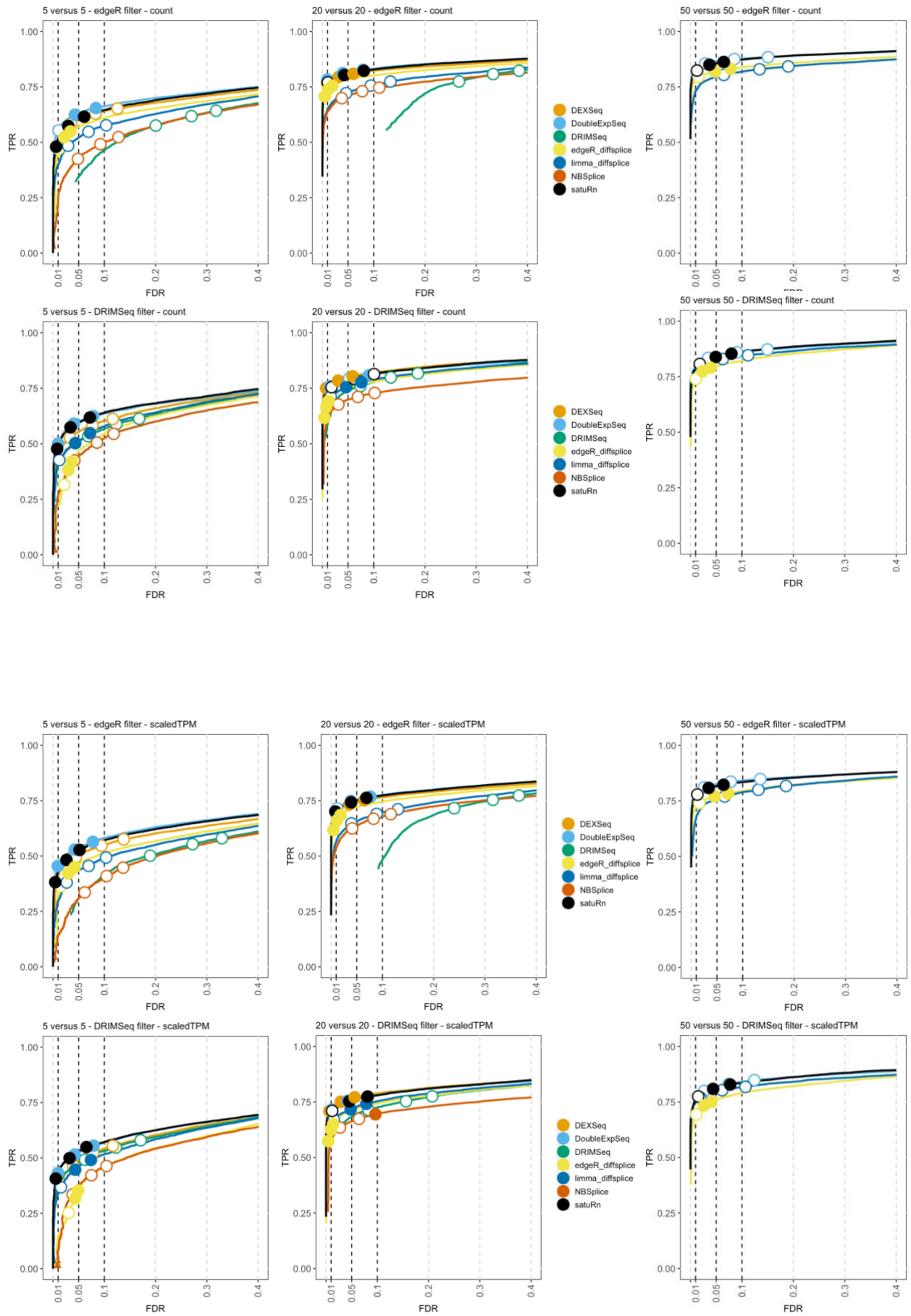
134
 135 **Figure S4: Performance evaluation of satuRn on the “Dmelanogaster” simulated bulk RNA-Seq dataset by Van**
 136 **den Berge et al.** FDR-TPR curves visualize the performance of each method by displaying the sensitivity of the
 137 method (TPR) with respect to the false discovery rate (FDR). The three circles on each curve represent working
 138 points when the FDR level is set at nominal levels of 1%, 5% and 10%, respectively. The circles are filled if the
 139 empirical FDR is equal or below the imposed FDR threshold. The benchmark was performed both on the raw
 140 counts (**row 1**) and on scaled TPM (**row 2**) as imported with the Bioconductor R package tximport¹. We
 141 additionally adopted two different filtering strategies; an edgeR-based filtering (**column 1**) and a DRIMSeq-based
 142 filtering (**column 2**). Overall, the performance of satuRn is on par with those of the best tools in the literature,
 143 DEXSeq and DoubleExpSeq. In contrast to the performance evaluation on the dataset by Love et al. (Figures 1A
 144 and S2), there is a limited difference in performances based on the data input type (i.e., counts versus scaled
 145 TPM), and DRIMSeq also performs well on these datasets.

146
 147
 148
 149
 150
 151
 152
 153

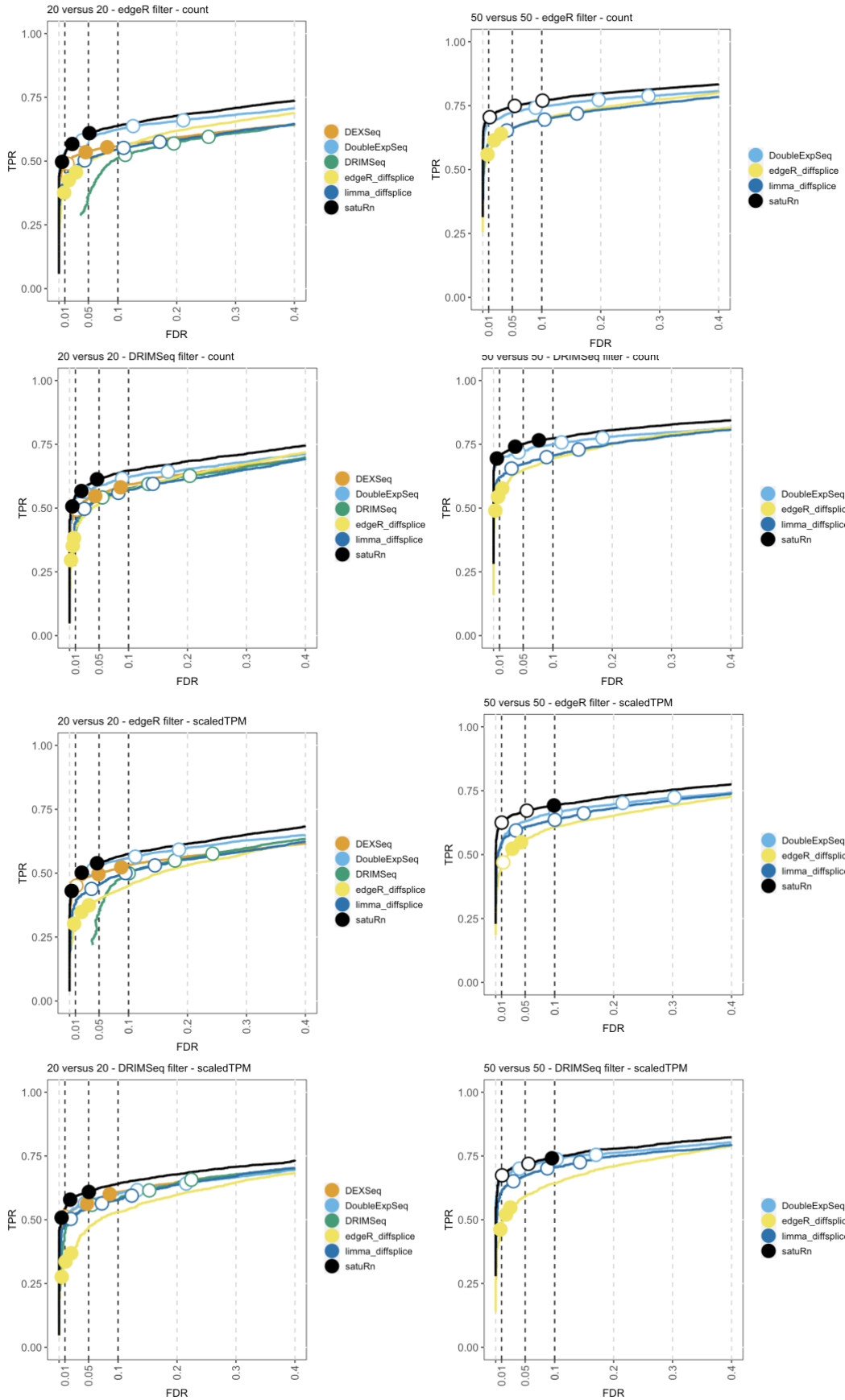


155
156
157
158
159
160
161
162
163
164
165
166
167
168
169
170
171

Figure S5: Performance evaluation of satuRn on the “Hsapiens” simulated bulk RNA-Seq dataset by Van den Berge et al. FDR-TPR curves visualize the performance of each method by displaying the sensitivity of the method (TPR) with respect to the false discovery rate (FDR). The three circles on each curve represent working points when the FDR level is set at nominal levels of 1%, 5% and 10%, respectively. The circles are filled if the empirical FDR is equal or below the imposed FDR threshold. The benchmark was performed both on the raw counts (**row 1**) and on scaled TPM (**row 2**) as imported with the Bioconductor R package tximport¹. We additionally adopted two different filtering strategies; an edgeR-based filtering (**column 1**) and a DRIMSeq-based filtering (**column 2**). Overall, the performance of satuRn is on par with those of the best tools in the literature, DEXSeq and DoubleExpSeq. In contrast to the performance evaluation on the dataset by Love et al. (Figures 1A and S2), there is a limited difference in performances based on the data input type (i.e., counts versus scaled TPM), and DRIMSeq also performs well on these datasets.



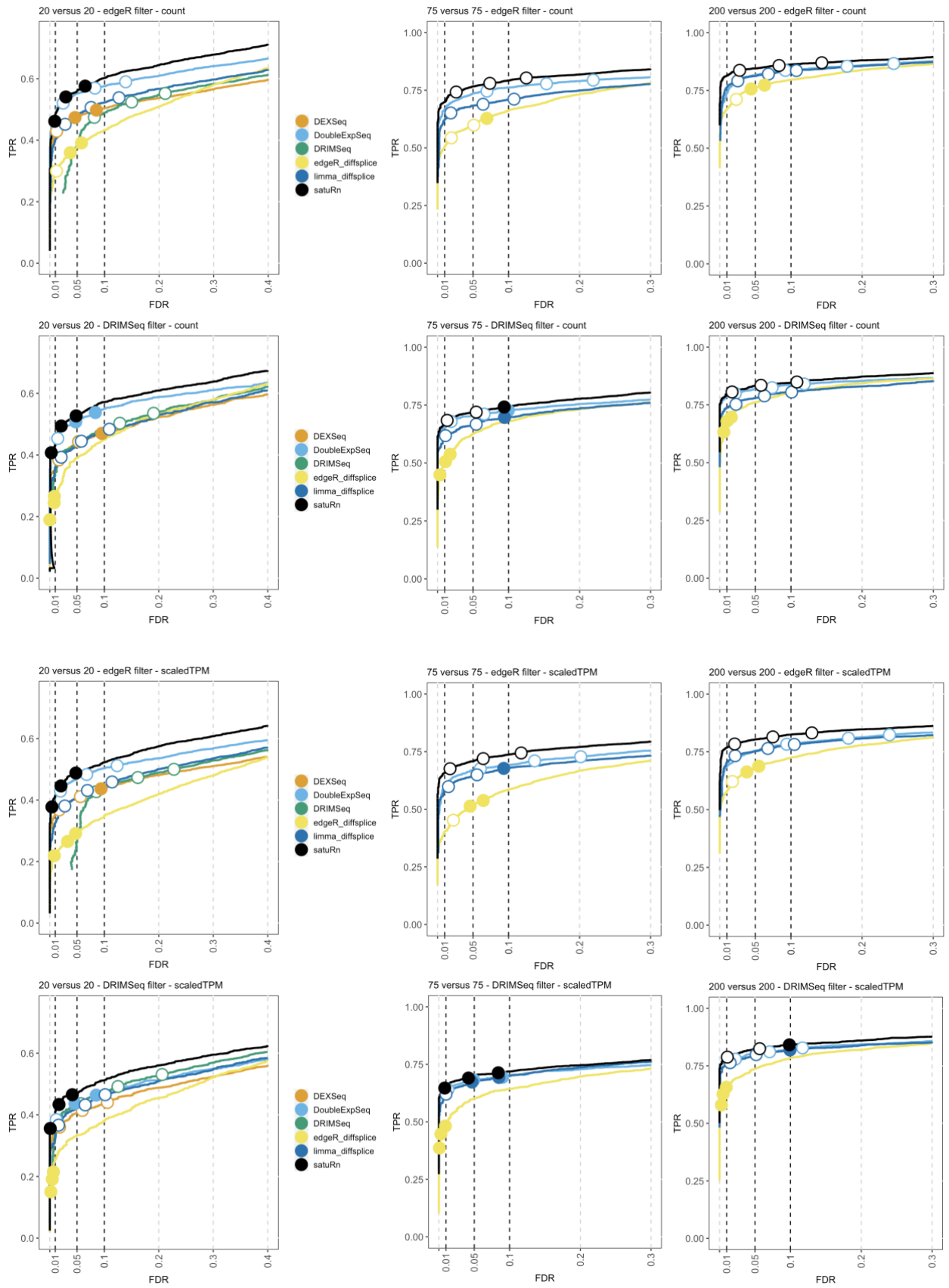
173 **Figure S6: Performance evaluation of satuRn on the GTEx bulk RNA-Seq dataset.** FDR-TPR curves visualize the
174 performance of each method by displaying the sensitivity (TPR) with respect to the false discovery rate (FDR).
175 The three circles on each curve represent working points when the FDR level is set at nominal levels of 1%, 5%
176 and 10%, respectively. The circles are filled if the empirical FDR is equal or below the imposed FDR threshold.
177 The benchmark was performed both on the raw counts (**rows 1 and 2**) or on scaled transcripts-per-million (TPM)
178 (**rows 3 and 4**) as imported with the Bioconductor R package tximport¹. We additionally adopted two different
179 filtering strategies; an edgeR-based filtering (**rows 1 and 3**) and a DRIMSeq-based filtering (**rows 2 and 4**). The
180 performance of satuRn is on par with the best tools from the literature, DEXSeq and DoubleExpSeq. In addition,
181 satuRn consistently provides a stringent control of the FDR, while DoubleExpSeq becomes more liberal with
182 increasing sample sizes. Note that DEXSeq, DRIMSeq and NBSplice were omitted from the largest comparison,
183 as these methods do not scale to large datasets (Figure1).
184
185
186
187
188
189
190
191
192
193
194
195
196
197
198
199
200
201
202
203
204
205
206
207
208
209
210
211
212
213
214
215
216
217
218
219
220
221
222
223
224
225
226
227



228
229

230 **Figure S7: Performance evaluation of satuRn on the real scRNA-Seq dataset by Chen et al.** FDR-TPR curves
231 visualize the performance of each method by displaying the sensitivity of the method (TPR) with respect to the
232 false discovery rate (FDR). The three circles on each curve represent working points when the FDR level is set at
233 nominal levels of 1%, 5% and 10%, respectively. The circles are filled if the empirical FDR is equal or below the
234 imposed FDR threshold. The benchmark was performed both on the raw counts (**rows 1 and 2**) or on scaled
235 transcripts-per-million (TPM) (**rows 3 and 4**) as imported with the Bioconductor R package tximport¹. We
236 additionally adopted two different filtering strategies; an edgeR-based filtering (**rows 1 and 3**) and a DRIMSeq-
237 based filtering (**rows 2 and 4**). The performance of satuRn is at least on par with the best tools from the
238 literature. Note that the performance of DEXSeq is clearly lower. In addition, our method consistently controls
239 the FDR close to its imposed nominal FDR threshold, while DoubleExpSeq becomes more liberal with increasing
240 sample sizes. DEXSeq and DRIMSeq were omitted from the largest comparison (two groups with 50 cells each),
241 as these methods do not scale to large datasets (Figure 1). NBSplice was omitted from all comparisons, as it does
242 not converge on datasets with many zeros, such as scRNA-Seq datasets.

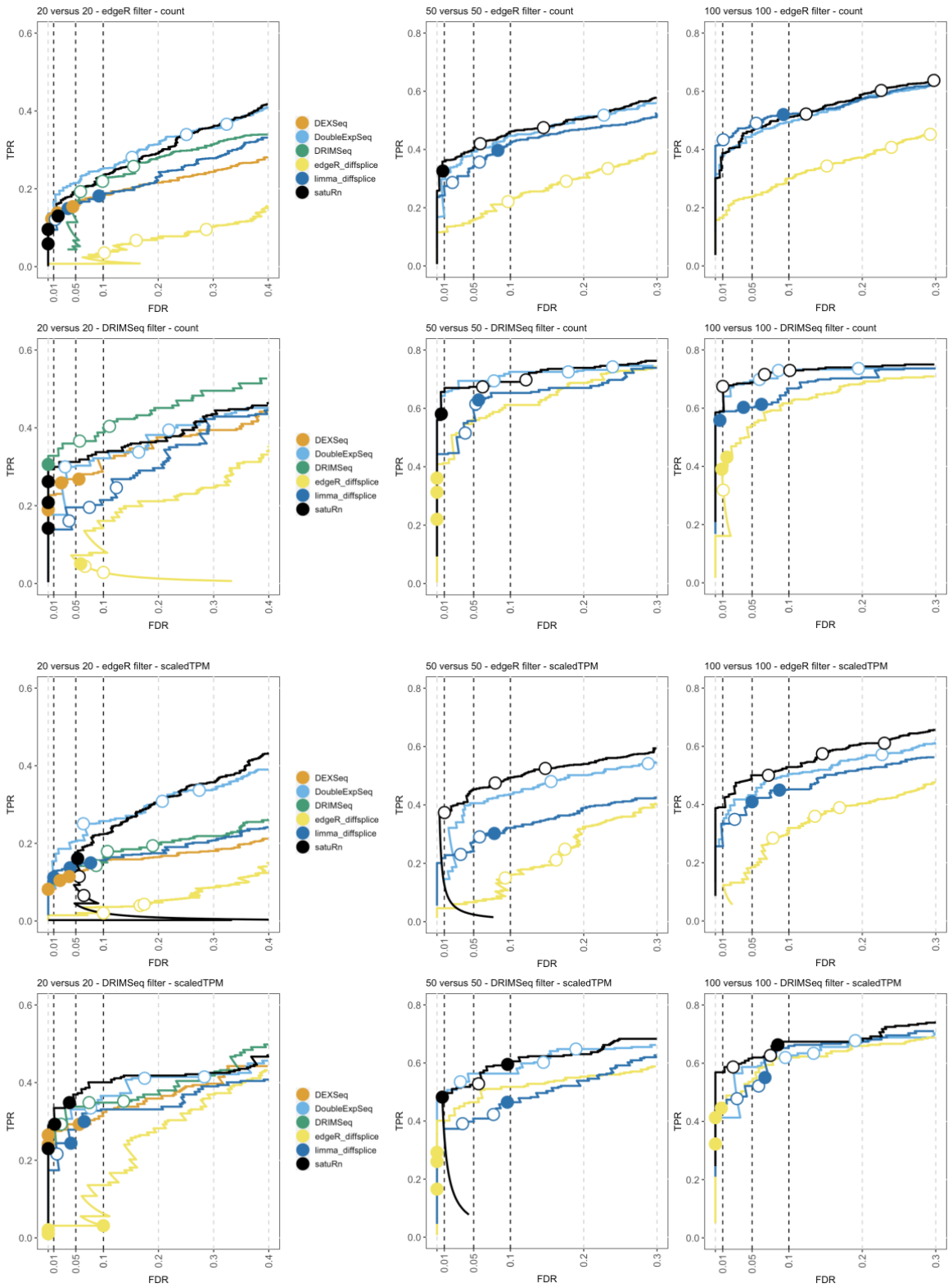
243
244
245
246
247
248
249
250
251
252
253
254
255
256
257
258
259
260
261
262



263
 264
 265
 266

267 **Figure S8: Performance evaluation of satuRn on the real scRNA-Seq dataset by Tasic et al.** FDR-TPR curves
268 visualize the performance of each method by displaying the sensitivity of the method (TPR) with respect to the
269 false discovery rate (FDR). The three circles on each curve represent working points when the FDR level is set at
270 nominal levels of 1%, 5% and 10%, respectively. The circles are filled if the empirical FDR is equal or below the
271 imposed FDR threshold. We generated three two-group comparisons of 20, 75 and 200 cells each (left, middle
272 and right panel, respectively). The benchmark was performed both on the raw counts (**rows 1 and 2**) or on scaled
273 transcripts-per-million (TPM) (**rows 3 and 4**) as imported with the Bioconductor R package tximport¹. We
274 additionally adopted two different filtering strategies; an edgeR-based filtering (**rows 1 and 3**) and a DRIMSeq-
275 based filtering (**rows 2 and 4**). Overall, satuRn slightly outperforms DoubleExpSeq, the best tools from the
276 literature. Note that the performance of DEXSeq is clearly lower. In addition, our method consistently controls
277 the FDR close to its imposed nominal FDR threshold, while DoubleExpSeq becomes more liberal with increasing
278 sample sizes. DEXSeq and DRIMSeq were omitted from the largest comparison (two groups with 75 cells and
279 200 cells each, respectively), as these methods do not scale to large datasets (Figure 1). NBSplice was omitted
280 from all comparisons, as it does not converge on datasets with many zeros, such as scRNA-Seq datasets.

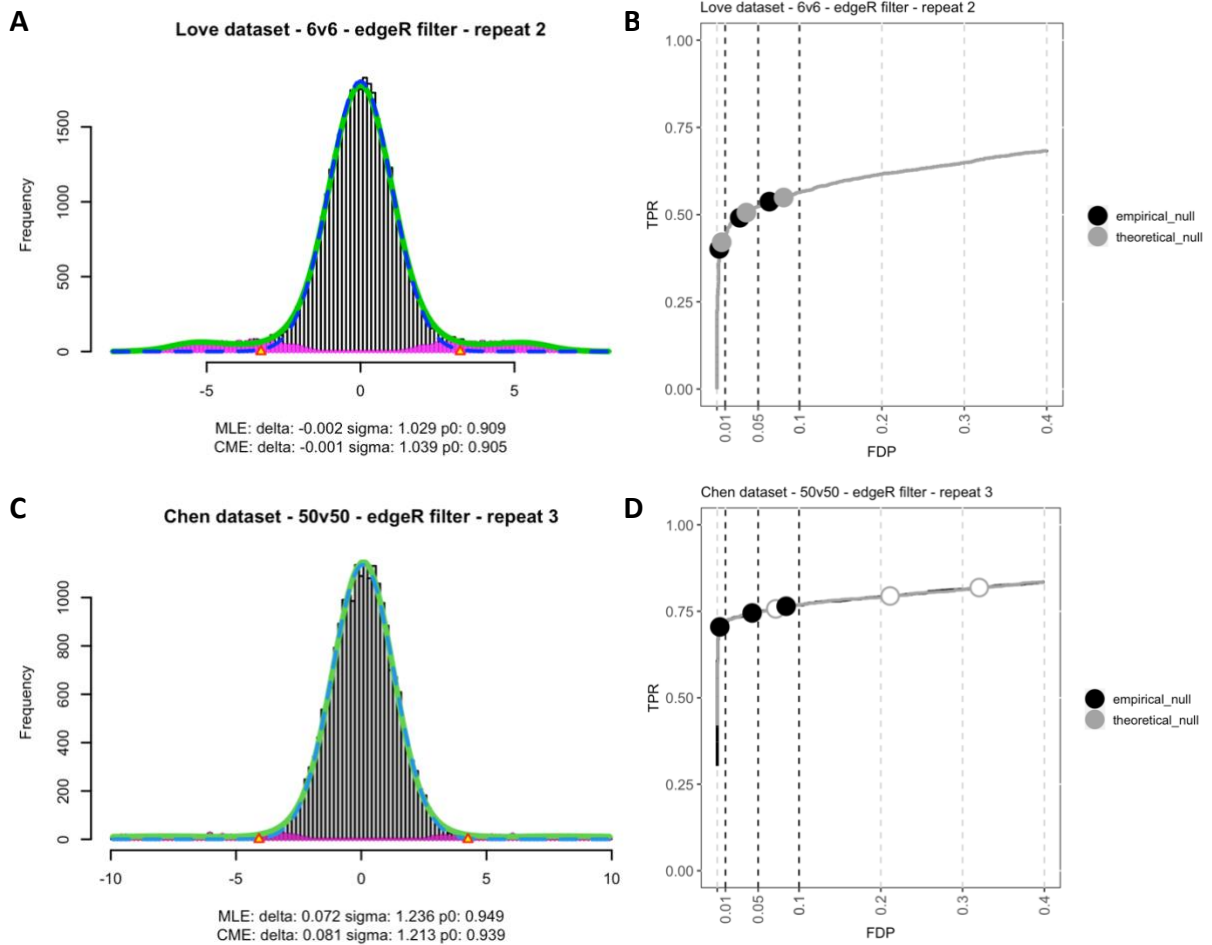
281
282
283
284
285
286
287
288
289
290
291
292
293
294
295
296
297
298
299
300
301
302
303
304
305
306
307
308
309
310
311
312
313
314
315



316
 317
 318
 319
 320
 321
 322

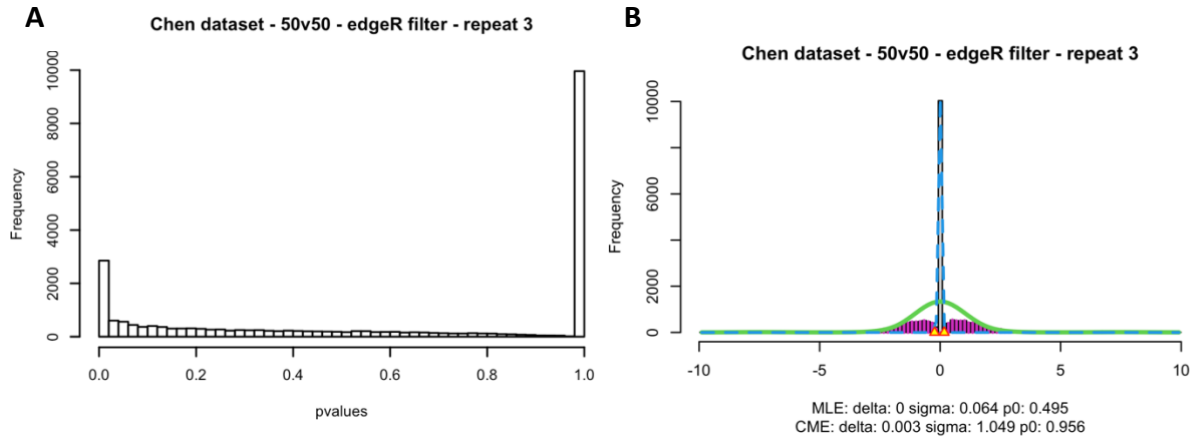
323 **Figure S9: Performance evaluation of satuRn on the real scRNA-Seq dataset by Darmanis et al.** FDR-TPR curves
324 visualize the performance of each method by displaying the sensitivity of the method (TPR) with respect to the
325 false discovery rate (FDR). The three circles on each curve represent working points when the FDR level is set at
326 nominal levels of 1%, 5% and 10%, respectively. The circles are filled if the empirical FDR is equal or below the
327 imposed FDR threshold. We generated three two-group comparisons of 20, 50 and 100 cells each (left, middle
328 and right panel, respectively). The benchmark was performed both on the raw counts (**rows 1 and 2**) or on scaled
329 transcripts-per-million (TPM) (**rows 3 and 4**) as imported with the Bioconductor R package tximport¹. We
330 additionally adopted two different filtering strategies; an edgeR-based filtering (**rows 1 and 3**) and a DRIMSeq-
331 based filtering (**rows 2 and 4**). Overall, the performance of satuRn is similar to DoubleExpSeq, the best tools
332 from the literature. In addition, our method consistently controls the FDR close to its imposed nominal FDR
333 threshold, while DoubleExpSeq becomes more liberal with increasing sample sizes. On the dataset with the
334 smallest sample size, the FDR control of *satuRn* does become too strict.

335
336
337
338
339
340
341
342
343
344
345
346
347
348
349
350
351
352
353
354
355
356
357
358
359
360
361
362
363
364
365
366
367
368
369
370
371



372
 373
 374
 375
 376
 377
 378
 379
 380
 381
 382
 383
 384
 385
 386
 387
 388
 389
 390
 391
 392
 393
 394

Figure S10: The effect of using an empirical null distribution on the false discovery control of satuRn. Panel A: Empirical distribution of the satuRn test statistics in one of the bulk transcriptomics benchmark datasets adapted from Love *et al.* The test statistics are z-scores, calculated from satuRn p-values as described in formula 5 (see Methods). As this benchmark dataset is constructed to have 15% DTU transcripts and thus 85% non-DTU or null transcripts, most of these z-scores are expected to follow a standard normal distribution (mean = 0, standard deviation = 1). This is reflected in the maximum likelihood estimates for the mean and variance of the empirical null distribution (mean = -0.002, standard deviation = 1.029). **Panel B:** Corresponding FDP-TPR curve for the bulk transcriptomics benchmark dataset. As the theoretical null distribution and the empirical null distribution are virtually identical, we observe a negligible difference between both strategies, both in terms of performance and FDP control. **Panel C:** Empirical distribution of the satuRn test statistics in one of the single-cell benchmark datasets adapted from Chen *et al.* Again, most of these z-scores are expected to follow a standard normal distribution as this benchmark dataset is also constructed to have 15% DTU transcripts and thus 85% non-DTU or null transcripts. However, the empirical distribution is considerably wider than expected (standard deviation = 1.236). We additionally observe a small shift of the distribution (mean = 0.072). **Panel D:** Corresponding FDP-TPR curve for the single-cell benchmark dataset. While the inference for satuRn is overly liberal when working under the theoretical null, FDP control is restored by adopting the wider empirical null distribution. Note that the performance will only be affected when the empirical null distribution is strongly shifted with respect to the theoretical null (i.e., a large mean in absolute value), which was not the case in this example nor in any other dataset from our analyses.



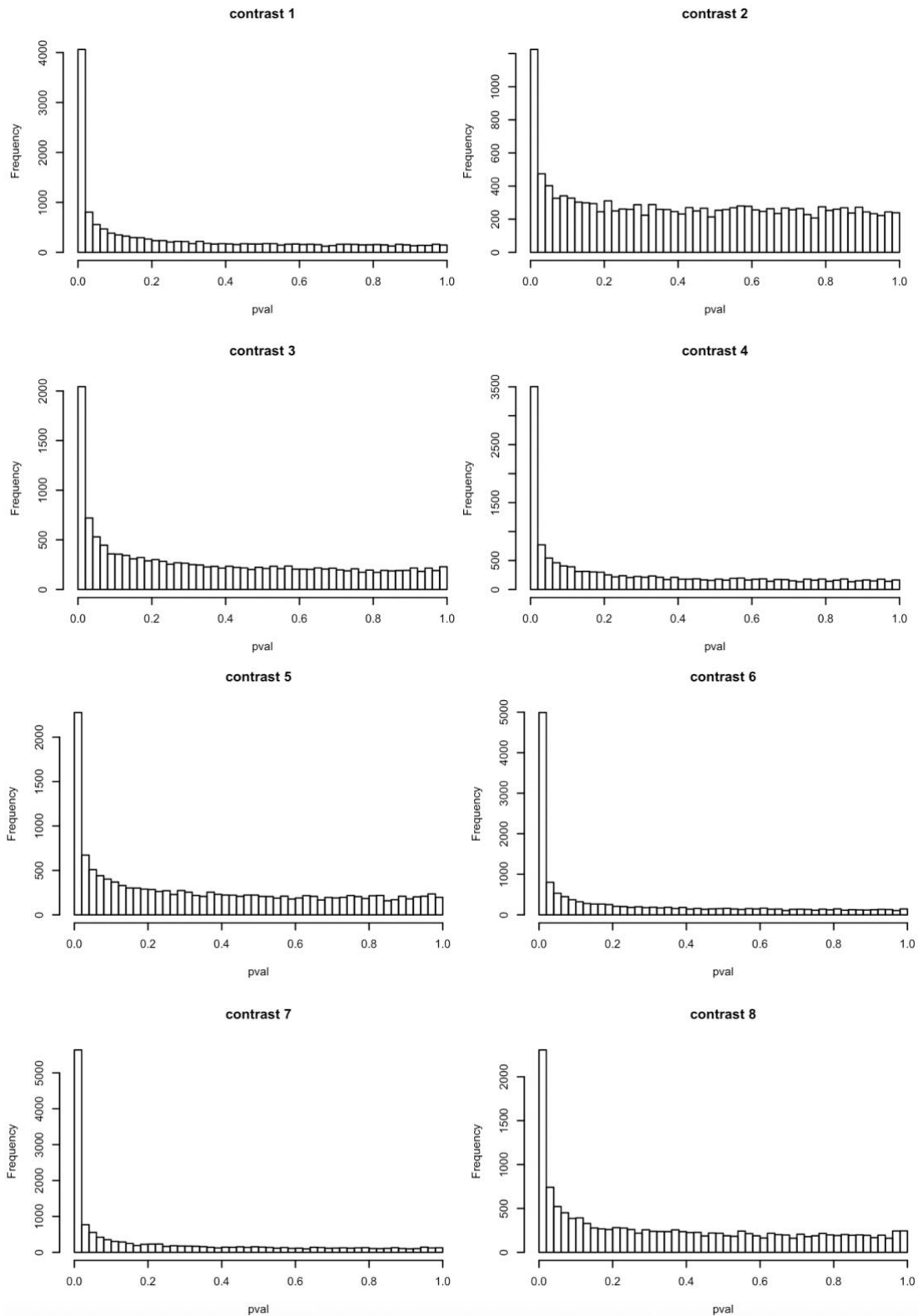
395
 396 **Figure S11: Adopting an empirical null distribution to improve FDR control is infeasible for DoubleExpSeq.**
 397 **Panel A:** Distribution of the p-values from a DoubleExpSeq analysis in one of the single-cell benchmark datasets
 398 adapted from Chen *et al.* We immediately observe the large spike of p-values equal to 1, which distorts the p-
 399 value distribution. In addition, the p-values in the mid-range (e.g., from 0.1 to 0.9), which are expected to be
 400 uniformly distributed, are skewed towards smaller values, which underlies the overly liberal results of
 401 DoubleExpSeq in our single-cell benchmarks. **Panel B:** The corresponding empirical distribution of the
 402 DoubleExpSeq test statistics. The test statistics are z-scores, calculated from the original DoubleExpSeq p-values
 403 as described in formula 5 (see Methods). As all our benchmark datasets are constructed to have 15% DTU
 404 transcripts and thus 85% non-DTU or null transcripts, most of these z-scores are expected to follow a standard
 405 normal distribution (mean = 0, standard deviation = 1). However, given the pathological distribution of the p-
 406 values it is not feasible to properly estimate the empirical null distribution, as also clearly shown by the widely
 407 different parameter estimates obtained using the two estimation frameworks implemented in the *locfdr* R
 408 package²; compare the estimates between MLE (maximum likelihood estimation) and CME (central matching
 409 estimation).

410
 411
 412
 413
 414
 415
 416
 417
 418
 419
 420
 421
 422
 423
 424
 425
 426
 427
 428
 429
 430
 431
 432

Comparison	Cell type 1 (ALM)	Cell type 2 (VlSp)	DoubleExpSeq FDR	Limma FDR	Limma Empirical FDR
1	Cpa6 Gpr88	Batf3	2142	3602	169
2	Cbln4 Fezf2	Col27a1	644	468	297
3	Cpa6 Gpr88	Col6a1 Fezf2	335	1029	77
4	Gkn1 Pcdh19	Col6a1 Fezf2	1878	2861	58
5	Lypd1 Gpr88	Hsd11b1 Endou	829	1411	249
6	Tnc	Hsd11b1 Endou	4580	4819	341
7	Tmem163 Dmrtb1	Hsd11b1 Endou	3388	5603	176
8	Tmem163 Arhgap25	Whrn Tox2	455	1387	166

433
434
435
436
437
438
439
440
441
442
443
444
445
446
447
448
449
450
451
452
453
454
455
456
457
458
459

Figure S12: Number of differentially used transcripts as identified by DoubleExpSeq and limma diffsplice. The first three columns indicate the comparisons between ALM cell types (column 2) and VlSp cell types (column 3), respectively. Column 4 indicates the number of differentially used transcripts as identified by DoubleExpSeq. Column 5 indicates the number of differentially used transcripts as identified by a limma diffsplice analysis with default settings. Column 6 displays the number of differentially used transcripts found by limma diffsplice after correcting for deviations between the theoretical and empirical null distributions.



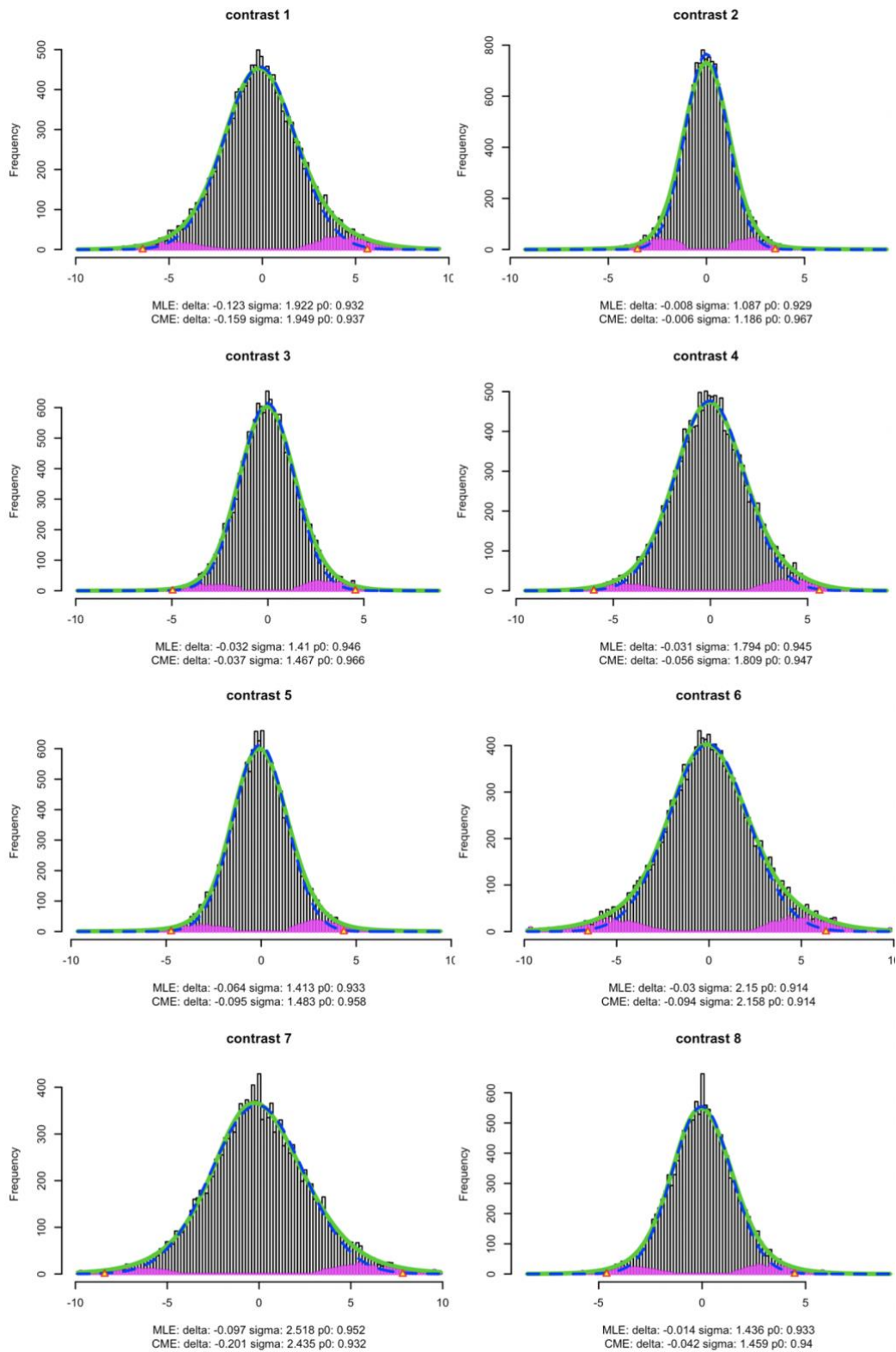
461

462

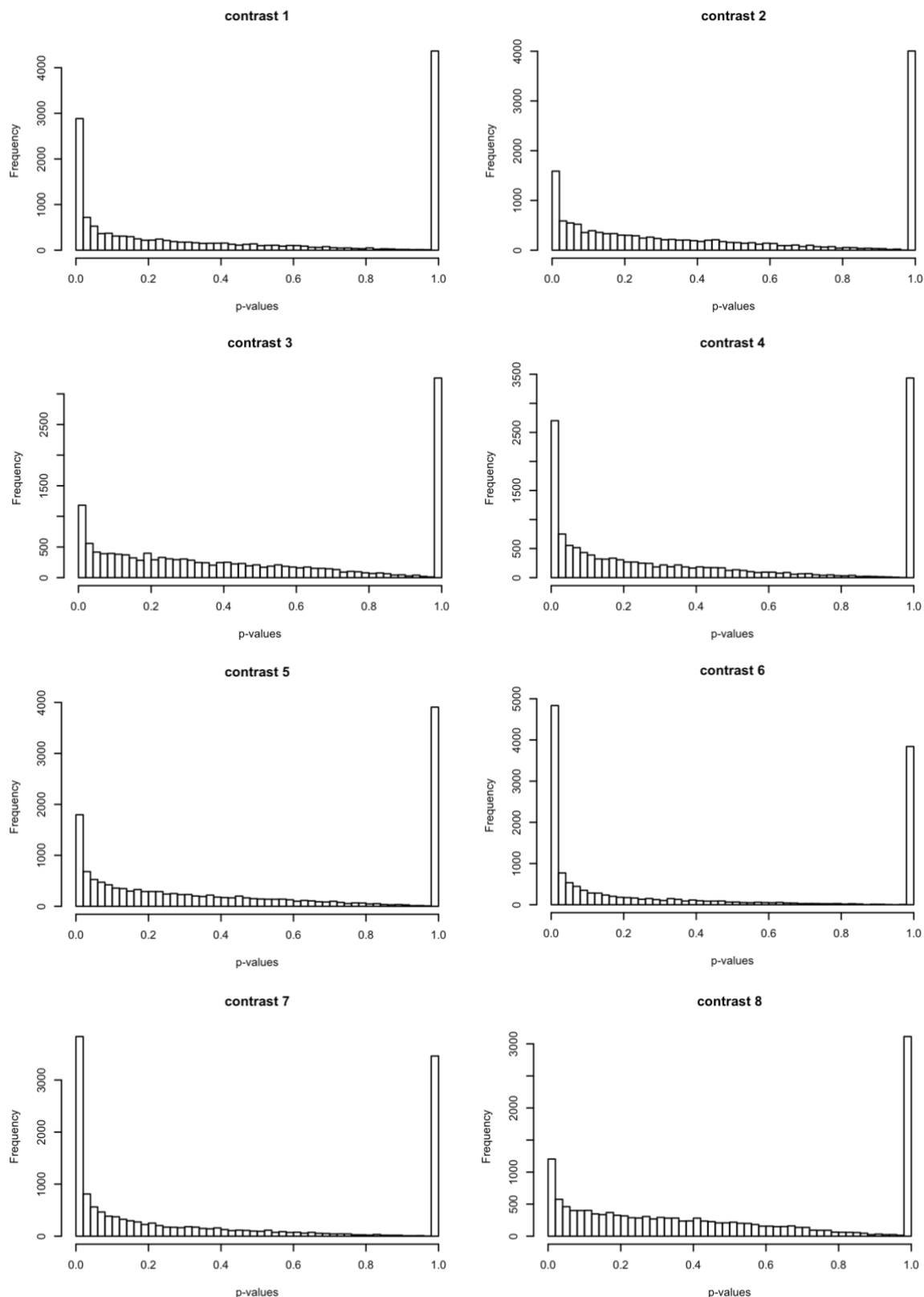
463 **Figure S13: Histograms of the p-values from limma diffsplice.** From these histograms, the huge number of DTU

464 transcripts identified by limma diffsplice become apparent. Note that the general tendency of limma diffsplice

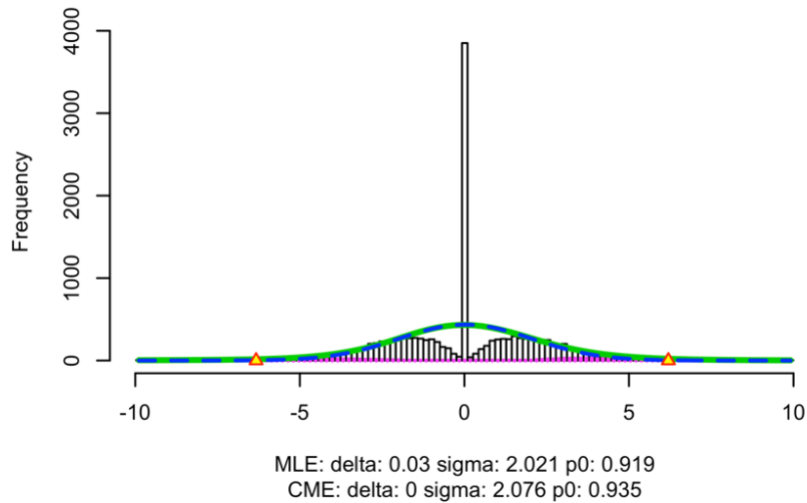
465 for smaller p-values is better visible when converting the p-values into z-scores (see Figure S13)



466 **Figure S14: Empirical distribution of the limma diffsplice test statistics.** The test statistics are z-scores,
 467 calculated from limma diffsplice p-values as described in formula 5. Theoretically, these z-scores are expected
 468 to follow a standard normal distribution (mean = 0, standard deviation =1). Here, however, the empirical
 469 distributions are considerably wider (standard deviation > 1), as indicated underneath the plots. This indicates
 470 that the results returned by limma diffsplice in this case study are overly liberal.



471
 472 **Figure S15: Histograms of the p-values from DoubleExpSeq.** From these histograms, the huge number of DTU
 473 transcripts identified by limma diffsplice become apparent. In addition, we observe a gradual decrease of p-
 474 values over the interval $[0.05 < p < 0.95]$, with a very large spike of p-values that are exactly 1 in all comparisons
 475 or contrasts of interest.



476
 477
 478
 479
 480
 481
 482
 483

Figure S16: Empirical distribution of the test statistics in comparison #6 of the case study with DoubleExpSeq. The test statistics are z-scores, calculated from DoubleExpSeq p-values as described in formula 5 (see Methods). Theoretically, the bulk of these z-scores are expected to follow a standard normal distribution (mean = 0, standard deviation = 1), i.e., assuming that most transcripts are not differentially used. However, the large spike of p-values equal to 1 (See Figure S14) results spike of z-scores equal to zero, which poses a problem when estimating the empirical null distribution (blue dashed curve).

484 References

485
 486
 487
 488
 489
 490

1. Sonesson, C., Love, M. I. & Robinson, M. D. Differential analyses for RNA-seq: transcript-level estimates improve gene-level inferences. *F1000Research* **4**, 1521 (2016).
2. Efron, B., Turnbull, B. B. & Narasimhan, B. Locfdr: Computes Local False Discovery Rates. *R Packag. Version 1.*, <http://CRAN.R-project.org/package=locfdr> (2011).